Asian Journal of Chemistry; Vol. 38, No. 9 (2026), 2419-2426
ASIAN JOURNAL OF CHEMISTRY
https://doi.org/10.14233/ajchem.2026.36472

Design, Synthesis and Anti-Breast Cancer Activity of New Benzimidazole-1,2,4-thiadiazoles-benzamide Hybrids

SARITHA SHEELAM[1,2] and JYOTHI MANDALA[1,*]

[1]Department of Chemistry, Mahatma Gandhi University, Nalgonda-508254, India
[2]Department of Chemistry, Govt. Polytechnic College for Women, Suryapet-508213, India

*Corresponding author: E-mail: jyothimandalamgu@gmail.com

Received: 20 May 2026 *Accepted*: 12 August 2026 *Published online*: 5 September 2026 AJC-22470

A new series of benzimidazole-1,2,4-thiadiazole-benzamide hybrids (**7a-l**) was synthesized and characterized. The synthesized hybrids were evaluated for anticancer activity against two breast cancer cell lines, MCF-7 and MDA-MB-231, using the MTT assay, with Erlotinib as the reference drug. The results revealed that hybrid **7i** exhibited more potent activity against both tested cancer cell lines than the standard drug Erlotinib. The other three hybrids, **7j**, **7k** and **7l**, displayed activity values close to that of the standard drug. Based on these findings, hybrids **7i**, **7j**, **7k** and **7l** were further evaluated for tyrosine kinase EGFR inhibitory activity using Erlotinib as the reference drug. Hybrids **7i** and **7j** exhibited higher EGFR inhibitory activity than erlotinib. Molecular docking studies of the potent hybrids with the EGFR receptor supported the biological results, with hybrids **7i** and **7l** exhibiting strong interactions with the EGFR protein and superior binding affinities compared with erlotinib. The combined anticancer, EGFR inhibitory and docking results identify hybrid **7i** as the most promising hybrid, while hybrids **7j** and **7l** represent potential EGFR-targeting anticancer candidates.

Keywords: Benzimidazolo-1,2,4-thiadiazolo-benzamide hybrids, Anticancer activity, EGFR activity, Molecular docking studies.

INTRODUCTION

Benzimidazole, 1,2,4-thiadiazole and benzamide are the key pharmacophores in medicinal chemistry, each associated with diverse biological activities. Benzimidazole has attracted particular attention owing to its structural resemblance to nucleotides present in biological systems and its cytotoxic activity against several cancer types [1-4]. Several benzimidazole-based compounds acting as tubulin-binding site inhibitors have undergone preclinical and clinical investigations for cancer treatment [5-8]. Their incorporation with other biologically relevant pharmacophores offers a rational strategy for developing new anticancer agents.

The benzamide moiety is widely encountered in naturally occurring pharmaceutically active compounds and constitutes an important structural element in numerous drugs and biologically active cyclic systems [9-12]. Medicinal chemistry analyses indicate that one or more amide bonds are present in nearly 25% of natural and synthetic pharmaceuticals [13-16]. The favourable biological compatibility and hydrogen bonding properties of amide groups have supported the development of amide-containing compounds as potential anticancer agents.

Thiadiazoles are five-membered sulphur- and nitrogen-containing heterocycles comprising four isomers viz. 1,2,3-thiadiazole, 1,2,4-thiadiazole, 1,2,5-thiadiazole and 1,3,4-thiadiazole [17]. Their bioisosteric relationship to pyrimidine and oxadiazole contributes to diverse pharmacological activities, for example, antiviral, antibacterial, antifungal, antiparasitic, anti-inflammatory and antitumour effects. Their mesoionic character favours membrane permeability, while the sulphur atom enhances lipophilicity. Clinically used thiadiazole containing drugs include acetazolamide, cefazedone, cefazolin sodium and methazolamide are already available in the market.

Cancer is a multifactorial disease involving complex interactions among environmental, genetic and epigenetic factors that regulate tumour development. It remains a major cause of mortality worldwide, accounting for approximately 8.8 million deaths according to the 2015 WHO assessment, with nearly 70% occurring in low- and middle-income countries [18-22]. The continuing cancer burden supports the develop-

ment of structurally diverse compounds with defined molecular targets.

The established biological relevance of benzimidazole, 1,2,4-thiadiazole and amide pharmacophores provides a basis for their molecular hybridization. In this work, these pharmacophores were integrated to design novel conjugates with potential EGFR inhibitory activity (Fig. 1). The synthesized compounds were evaluated for *in vitro* anticancer activity, followed by EGFR inhibition studies on the active derivatives. Potent compounds were subjected to in silico molecular docking studies to characterize their interactions with the EGFR binding site and rationalize their biological activity [23,24].

EXPERIMENTAL

Laboratory grade chemicals were purchased from the Sigma-Aldrich Company. Merck silica gel plates are having a mesh size of 60-120 for column chromatography and precoating $60F_{254}$ for TLC. The compounds melting points were ascertained by using the Casia-Siamia (VMP-AM) melting point equipment. Using a Bruker 100 MHz spectrometer, ^{13}C NMR spectra were acquired with DMSO as the solvent and TMS as the reference. Spectrometer Varian Gemini 400 MHz was used to acquire ^{1}H NMR spectra. A Shimadzu QP5050A quadrupole mass spectrometer was used to find the EI mass spectra (at an ionizing voltage of 70 eV).

Synthesis of 3-(1*H*-benzo[*d*]imidazol-1-yl)propane nitrile (3): In a clean round-bottom flask, benzimidazole (**1**, 5.0 g, 43 mmol) was dissolved in acetonitrile (20 mL) and stirred for 10 min at room temperature followed by the addition of K_2CO_3 (8.76 g, 64 mmol) and the mixture was stirred for a further 30 min. 3-Bromopropanenitrile (**2**, 5.66 g, 43 mmol) was then added dropwise and the reaction mixture was refluxed for 2 h. Reaction progress was monitored by TLC. After completion, the mixture was diluted with water (20 mL) and extracted with ethyl acetate (2 × 20 mL). The combined organic layers were washed with brine, filtered, concentrated under reduced pressure and then dried over anhydrous Na_2SO_4.

Synthesis of 3-(2-(1*H*-benzo[*d*]imidazol-1-yl)ethyl)-1,2,4-thiadiazol-5-amine (5): 3-(1*H*-Benzo[*d*]imidazol-1-yl)-propane nitrile (**3**, 1.2g, 48 mmol), $AlCl_3$ (0.64 g, 48 mmol) and *n*-butyl acetate (10 mL) were added to a clean 100 mL round bottom flask and the reaction mixture was stirred at room temperature for 20 min. Thiourea (**4**, 57 mmol, 0.43 g) was then added portion-wise to the reaction mixture, which was heated at 70 °C for 6 h. The reaction mixture was cooled to room temperature and water (0.5 mL) and iodine (12 mmol, 0.30 g) were added. The reaction mixture was then stirred for 24 h at room temperature. The progress of the reaction was monitored by TLC. After completion, the reaction was quenched with a saturated solution of $Na_2S_2O_3$. The reaction mixture was extracted with water and ethyl acetate (3 × 10 mL). The combined organic layers were dried over anhydrous Na_2SO_4, concentrated and purified by column chromatography on silica gel using petroleum ether/EtOAc as the eluent.

General synthesis of benzimidazole-1,2,4-thiadiazole-benzamide hybrids (7a-l): In a clean round-bottom flask, a

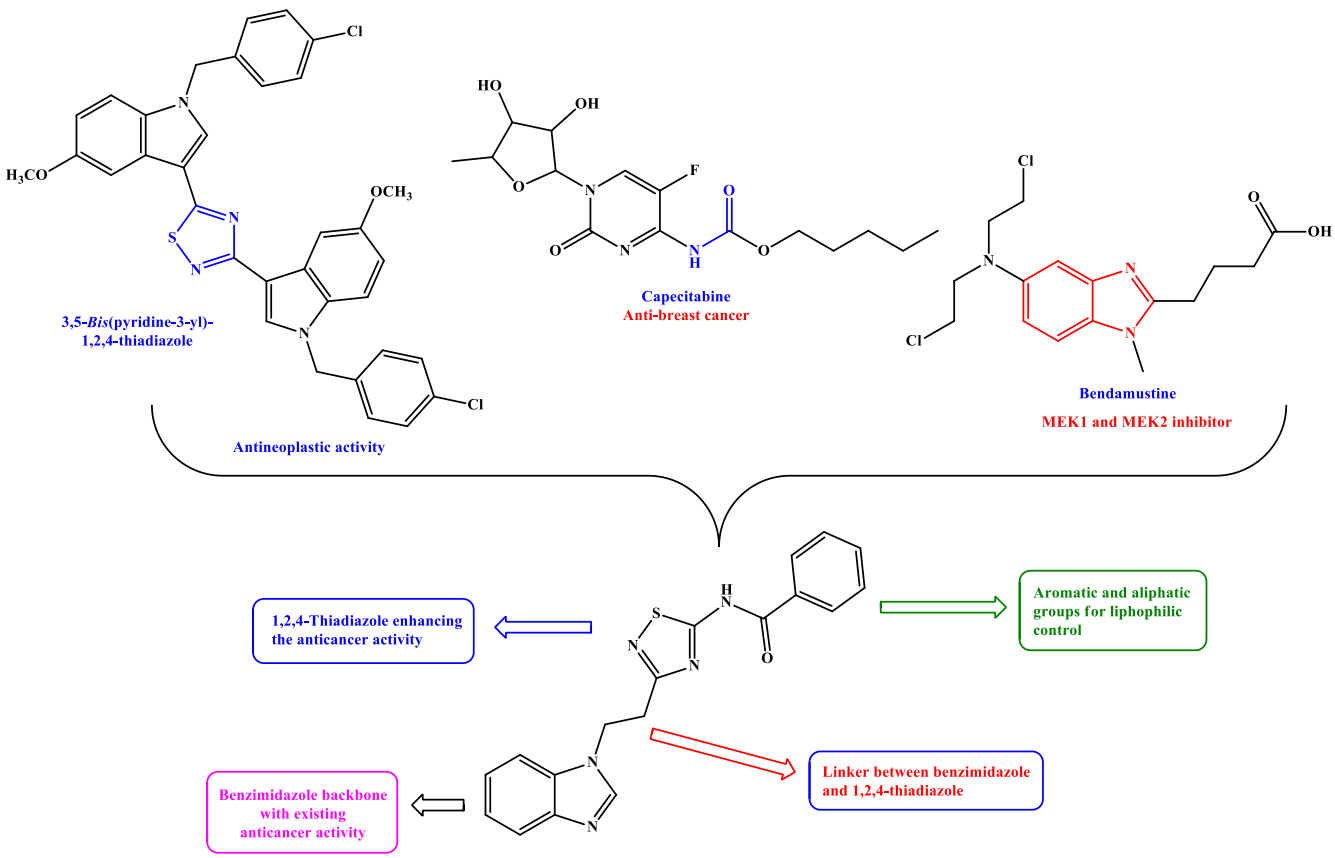

Fig. 1. Pharmacophore hybridization of benzimidazole-1,2,4-thiadiazole benzamide hybrids (**7a-l**)

mixture of 3-(2-(1*H*-benzo[*d*]imidazol-1-yl)ethyl)-1,2,4-thiadiazol-5-amine (**5**, 38 mmol, 0.90 g), benzoic acid (**6a**, 38 mmol, 0.46 g), EDCI (36 mmol, 0.72 g) and HOBt (34 mmol, 0.51 g) was dissolved in 20 mL of dry dichloromethane and stirred at room temperature for 6 h. The progress of the reaction was monitored by TLC. After completion, the reaction mixture was diluted with dichloromethane and washed with a saturated solution of $NaHCO_3$, filtered, the organic layer was concentrated under vacuum dried over anhydrous Na_2SO_4 (**Scheme-I**) The crude product was purified by column chromatography using ethyl acetate/hexane (4:6) as an eluent to give the corresponding pure product.

The remaining hybrids were synthesized by following the same procedure (**7b-l**).

***N*-(3-(2-(1*H*-Benzo[*d*]imidazol-1-yl)ethyl)-1,2,4-thiadiazol-5-yl)benzamide (7a):** Light brown solid; yield: 79%; m.p.: 217-219 ºC; ^{1}H NMR (400 MHz, DMSO-d_6, δ ppm): 11.20 (s, 1H), 8.10 (s, 1H), 7.89-7.81 (m, 4H), 7.63-7.56 (m, 5H), 4.17 (t, *J* = 3.8 Hz, 2H, -CH_2-), 3.40 (t, *J* = 3.8 Hz, 2H, -CH_2-); ^{13}C NMR (100 MHz, DMSO-d_6, δ ppm): 171.4, 167.2, 163.5, 149.2, 144.3, 137.4, 136.5, 133.4, 131.5, 130.2, 125.4, 124.6, 121.4, 112.3, 44.5, 28.4; MS (ESI): *m/z* 350 $[M+H]^+$; Anal. calcd. (found) % for $C_{18}H_{15}N_5OS$: C, 61.87 (61.85); H, 4.33 (4.31); N, 20.04 (20.02).

***N*-(3-(2-(1H-Benzo[*d*]imidazol-1-yl)ethyl)-1,2,4-thiadiazol-5-yl)-4-methylbenzamide (7b):** Light white solid; yield: 81%; m.p.: 221-223 ºC; ^{1}H NMR (400 MHz, DMSO-d_6, δ ppm): 11.19 (s, 1H), 8.07 (s, 1H), 7.86-7.78 (m, 4H), 7.61 (d, 2H, *J* = 4.8 Hz), 7.54 (d, 2H, *J* = 4.6 Hz), 4.15 (t, *J* = 3.4 Hz, 2H, -CH_2-), 3.37 (t, *J* = 3.3 Hz, 2H, -CH_2-), 2.40 (s, 3H); ^{13}C NMR (100 MHz, DMSO-d_6, δ ppm): 171.0, 169.2, 163.5, 149.4, 143.5, 142.4, 136.5, 134.3, 131.2, 130.4, 125.6, 124.1, 121.1, 112.1, 44.2, 28.1, 23.5; MS (ESI): *m/z* 364 $[M+H]^+$; Anal. calcd. (found) % for $C_{19}H_{17}N_5OS$: C, 62.79 (62.75); H, 4.71 (4.70); N, 19.27 (19.26).

***N*-(3-(2-(1*H*-Benzo[*d*]imidazol-1-yl)ethyl)-1,2,4-thiadiazol-5-yl)-3-methylbenzamide (7c):** Whitish solid; yield: 77%; m.p.: 227-229 ºC; ^{1}H NMR (400 MHz, DMSO-d_6, δ ppm): 11.21 (s, 1H), 8.09 (s, 1H), 7.90-7.83 (m, 4H), 7.64-7.57 (m, 3H), 7.46 (s, 1H), 4.19 (t, *J* = 3.7 Hz, 2H, -CH_2-), 3.42 (t, *J* = 3.6 Hz, 2H, -CH_2-), 2.42 (s, 3H); ^{13}C NMR (100 MHz, DMSO-d_6, δ ppm): 170.4, 166.2, 163.4, 148.4, 141.3, 140.6, 136.4, 135.4, 133.5, 130.3, 129.5, 128.6, 124.6, 124.5, 123.1, 121.5, 112.6, 44.6, 28.3, 23.8; MS (ESI): *m/z* 364 $[M+H]^+$; Anal. calcd. (found) % for $C_{19}H_{17}N_5OS$: C, 62.79 (62.77); H, 4.71 (4.69); N, 19.27 (19.25).

***N*-(3-(2-(1*H*-Benzo[*d*]imidazol-1-yl)ethyl)-1,2,4-thiadiazol-5-yl)-3,5-dimethylbenzamide (7d):** Light brown solid; yield: 82%; m.p.: 217-219 ºC; ^{1}H NMR (400 MHz, DMSO-d_6, δ ppm): 11.14 (s, 1H), 8.06 (s, 1H), 7.84-7.76 (m, 4H), 7.59 (s, 2H), 7.52 (s, 1H), 4.18 (t, *J* = 3.8 Hz, 2H, -CH_2-), 3.42 (t, *J* = 3.7 Hz, 2H, -CH_2-), 2.38 (s, 6H); ^{13}C NMR (100 MHz, DMSO-d_6, δ ppm): 170.6, 168.7, 163.3, 149.8, 142.6, 140.1, 137.4, 136.6, 135.6, 129.3, 126.2, 124.2, 120.8, 118.8, 44.2, 27.9, 23.2; MS (ESI): *m/z* 378 $[M+H]^+$; Anal. calcd. (found) % for $C_{20}H_{19}N_5OS$: C, 63.64 (63.63); H, 5.07 (5.05); N, 18.55 (18.54).

***N*-(3-(2-(1*H*-Benzo[*d*]imidazol-1-yl)ethyl)-1,2,4-thiadiazol-5-yl)-4-methoxybenzamide (7e):** Light cream solid; yield: 86%; m.p.: 204-206 ºC; ^{1}H NMR (400 MHz, DMSO-d_6, δ ppm): 11.06 (s, 1H), 7.98 (s, 1H), 7.76-7.69 (m, 4H), 7.53 (d, 2H, *J* = 5.8 Hz), 7.44 (d, 2H, *J* = 5.7 Hz), 4.10 (t, *J* = 3.4 Hz, 2H, -CH_2-), 3.93 (s, 3H), 3.39 (t, *J* = 3.4 Hz, 2H, -CH_2-); ^{13}C NMR (100 MHz, DMSO-d_6, δ ppm): 169.5, 166.5,

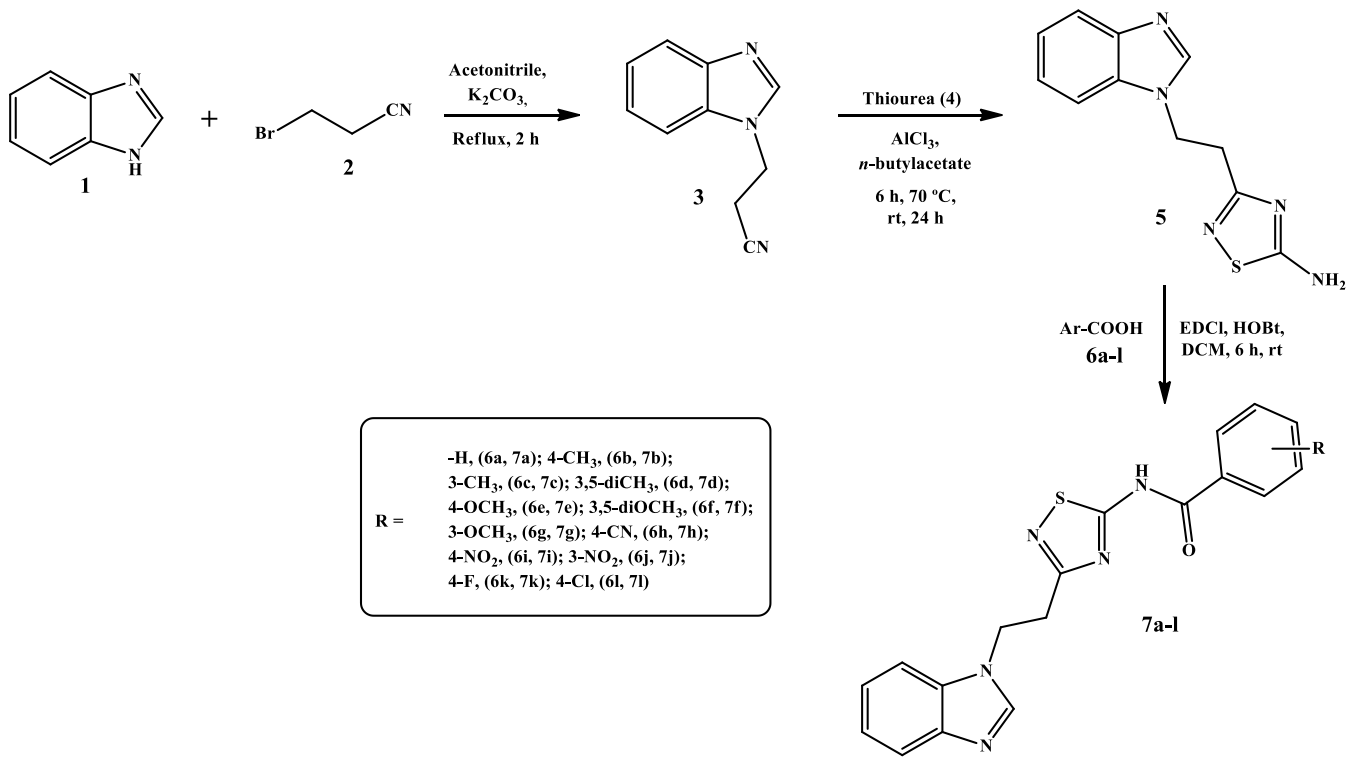

Scheme-I: Synthesis of benzimidazolo-1,2,4-thiadiazolo-benzamide hybrids (**7a-l**)

163.5, 162.4, 149.2, 143.2, 136.3, 130.3, 129.4, 125.1, 123.1, 120.3, 114.5, 112.1, 58.4, 43.3, 27.8; MS (ESI): *m/z* 380 $[M+H]^+$; Anal. calcd. (found) % for $C_{19}H_{17}N_5O_2S$: C, 60.14 (60.13); H, 4.52 (4.50); N, 18.46 (18.45).

***N*-(3-(2-(1*H*-Benzo[*d*]imidazol-1-yl)ethyl)-1,2,4-thiadiazol-5-yl)-3,5-dimethoxy benzamide (7f):** Light brown solid; yield: 88%; m.p.: 208-210 ºC; ^{1}H NMR (400 MHz, DMSO-d_6, δ ppm): 11.04 (s, 1H), 7.97 (s, 1H), 7.74-7.67 (m, 4H), 7.52 (s, 2H), 7.42 (s, 1H), 4.08 (t, *J* = 3.2 Hz, 2H, -CH_2-), 3.40 (t, *J* = 3.1 Hz, 2H, -CH_2-), 3.90 (s, 6H); ^{13}C NMR (100 MHz, DMSO-d_6, δ ppm): 169.3, 166.2, 162.8, 161.3, 149.7, 143.1, 137.4, 136.2, 125.3, 123.6, 119.5, 111.6, 109.4, 107.4, 57.6, 43.9, 28.3; MS (ESI): *m/z* 410 $[M+H]^+$; Anal. calcd. (found) % for $C_{20}H_{19}N_5O_3S$: C, 58.67 (58.65); H, 4.68 (4.66); N, 17.10 (17.08).

***N*-(3-(2-(1*H*-Benzo[*d*]imidazol-1-yl)ethyl)-1,2,4-thiadiazol-5-yl)-3-methoxybenzamide (7g):** Whitish solid; yield: 84%; m.p.: 214-216 ºC; ^{1}H NMR (400 MHz, DMSO-d_6, δ ppm): 11.09 (s, 1H), 8.06 (s, 1H), 7.79-7.72 (m, 4H), 7.54-7.46 (m, 3H), 7.42 (s, 1H), 4.14 (t, *J* = 3.4 Hz, 2H, -CH_2-), 3.39 (t, *J* = 3.3 Hz, 2H, -CH_2-), 3.94 (s, 3H); ^{13}C NMR (100 MHz, DMSO-d_6, δ ppm): 170.6, 167.5, 163.2, 161.5, 149.5, 144.6, 137.3, 136.3, 129.4, 125.2, 123.3, 122.2, 120.5, 117.2, 116.5, 112.4, 58.4, 43.7, 28.3; MS (ESI): *m/z* 380 $[M+H]^+$; Anal. calcd. (found) % for $C_{19}H_{17}N_5O_2S$: C, 60.14 (60.12); H, 4.52 (4.49); N, 18.46 (18.44).

***N*-(3-(2-(1*H*-Benzo[*d*]imidazol-1-yl)ethyl)-1,2,4-thiadiazol-5-yl)-4-cyanobenzamide (7h):** Light white solid; yield: 74%; m.p.: 227-229 ºC; ^{1}H NMR (400 MHz, DMSO-d_6, δ ppm): 11.15 (s, 1H), 8.10 (s, 1H), 7.96 (d, 2H, *J* = 5.4 Hz), 7.89-7.81 (m, 4H), 7.68 (d, 2H, *J* = 5.4 Hz), 4.22 (t, *J* = 4.4 Hz, 2H, -CH_2-), 3.45 (t, *J* = 4.4 Hz, 2H, -CH_2-); ^{13}C NMR (100 MHz, DMSO-d_6, δ ppm): 172.1, 168.4, 163.5, 149.7, 144.2, 141.2, 136.5, 134.3, 132.4, 125.3, 124.0, 121.4, 121.0, 117.5, 113.3, 44.7, 28.7; MS (ESI): *m/z* 375 $[M+H]^+$; Anal. calcd. (found) % for $C_{19}H_{14}N_6OS$: C, 60.95 (60.93); H, 3.77 (3.75); N, 22.45 (22.44).

***N*-(3-(2-(1*H*-Benzo[*d*]imidazol-1-yl)ethyl)-1,2,4-thiadiazol-5-yl)-4-nitrobenzamide (7i):** Light yellow solid; yield: 64%; m.p.: 211-213 ºC; ^{1}H NMR (400 MHz, DMSO-d_6, δ ppm): 11.30 (s, 1H), 8.41 (d, 2H, *J* = 6.2 Hz), 8.23 (d, 2H, *J* = 6.2 Hz), 8.14 (s,1H), 7.93-7.86 (m, 4H), 4.30 (t, *J* = 5.1 Hz, 2H, -CH_2-), 3.41 (t, *J* = 5.0 Hz, 2H, -CH_2-); ^{13}C NMR (100 MHz, DMSO-d_6, δ ppm): 172.9, 169.4, 164.5, 152.4, 150.5, 143.5, 141.6, 136.4, 132.7, 127.2, 125.4, 124.5, 122.5, 113.5, 45.5, 28.6; MS (ESI): *m/z* 395 $[M+H]^+$; Anal. calcd. (found) % for $C_{18}H_{14}N_6O_3S$: C, 54.82 (54.80); H, 3.58 (3.56); N, 21.31 (21.30).

***N*-(3-(2-(1*H*-Benzo[*d*]imidazol-1-yl)ethyl)-1,2,4-thiadiazol-5-yl)-3-nitrobenzamide (7j):** Light yellow solid; yield: 61%; m.p.: 226-228 ºC; ^{1}H NMR (400 MHz, DMSO-d_6, δ ppm): 11.37 (s, 1H), 8.82 (s, 1H), 8.24-8.19 (m, 3H), 8.12 (s, 1H), 7.89-7.82 (m, 4H), 4.32 (t, *J* = 5.4 Hz, 2H, -CH_2-), 3.43 (t, *J* = 5.4 Hz, 2H, -CH_2-); ^{13}C NMR (100 MHz, DMSO-d_6, δ ppm): 173.2, 169.7, 164.6, 151.4, 149.5, 143.4, 139.5, 136.6, 135.3, 131.5, 129.7, 126.6, 125.3, 124.1, 121.3, 114.2, 46.2, 28.7; MS (ESI): *m/z* 395 $[M+H]^+$; Anal. calcd. (found) % for $C_{18}H_{14}N_6O_3S$: C, 54.82 (54.81); H, 3.58 (3.55); N, 21.31 (21.28).

***N*-(3-(2-(1*H*-Benzo[*d*]imidazol-1-yl)ethyl)-1,2,4-thiadiazol-5-yl)-4-fluorobenzamide (7k):** Brown solid; yield: 65%; m.p.: 215-217 ºC; ^{1}H NMR (400 MHz, DMSO-d_6, δ ppm): 11.19 (s, 1H), 8.05 (s, 1H), 7.89 (d, 2H, *J* = 7.8 Hz), 7.82-7.76 (m, 4H), 7.64 (d, 2H, *J* = 7.7 Hz), 4.27 (t, *J* = 4.2 Hz, 2H, -CH_2-), 3.36 (t, *J* = 4.2 Hz, 2H, -CH_2-); ^{13}C NMR (100 MHz, DMSO-d_6, δ ppm): 169.4, 168.3, 166.4, 164.2, 163.4, 149.2, 143.4, 136.2, 132.3, 131.4, 125.5, 123.4, 120.2, 117.5, 116.2, 115.3, 114.7, 112.2, 44.2, 27.5; MS (ESI): *m/z* 368 $[M+H]^+$; Anal. calcd. (found) % for $C_{18}H_{14}FN_5OS$: C, 58.85 (58.83); H, 3.84 (3.82); N, 19.06 (19.05).

***N*-(3-(2-(1*H*-Benzo[*d*]imidazol-1-yl)ethyl)-1,2,4-thiadiazol-5-yl)-4-chlorobenzamide (7l):** White solid; yield: 67%; m.p.: 220-222 ºC; ^{1}H NMR (400 MHz, DMSO-d_6, δ ppm): 11.17 (s, 1H), 8.04 (s, 1H), 7.82 (d, 2H, *J* = 6.4 Hz), 7.76-7.69 (m, 4H), 7.62 (d, 2H, *J* = 6.3 Hz), 4.31 (t, *J* = 3.9 Hz, 2H, -CH_2-), 3.38 (t, *J* = 4.0 Hz, 2H, -CH_2-); ^{13}C NMR (100 MHz, DMSO-d_6, δ ppm): 169.1, 167.8, 166.1, 163.2, 148.7, 143.2, 135.9, 132.1, 130.8, 125.2, 123.1, 119.8, 117.2, 111.8, 45.2, 28.2; MS (ESI): *m/z* 384 $[M+H]^+$, 386 [M+2]; Anal. calcd. (found) % for $C_{18}H_{14}ClN_5OS$: C, 56.32 (56.30); H, 3.68 (3.67); N, 18.25 (18.23).

MTT assay: *In vitro* anticancer activity was tested using MTT colorimetric assay as per ATCC protocol. Cell lines that were used for testing *in vitro* cytotoxicity included MCF-7 and MDA-MB-231 Cell lines were maintained at 37 ºC in a humidified 5% CO_2 incubator using suitable media prescribed in NCCS Protocol. Decontaminated flasks were incubated for subculture. Cells were passed by 12 numbers. After getting 70% confluence; from culture flasks take 100 µL cell suspension and make a cell count using haemocytometer and found 5000-6000 per well in a 96-well plate. Cell suspension was mixed thoroughly by pip petting several times to get a uniform single cell suspension. Different dilutions of drugs solutions 3, 10, 30, 100 µM were prepared in media with final 0.5% DMSO. Cell suspension (100 µL) was aseptically dispensed into each well of a 96-well plate, followed by 100 µL of drug solution in culture medium in quadruplicate. The plate was incubated at 37 ºC in a CO_2 incubator. After 48 h, 20 µL of MTT solution was added to each well and incubated for a further 2 h. Subsequently, 80 µL of analysis buffer was added, and the plate was wrapped in aluminium foil to protect the dye from oxidation and placed on a shaker for 30 min. The absorbance was recorded on the ELISA reader (Biotech EL × 800) at 570 nm wavelength. The % inhibition was calculated by following formula:

$$\text{Inhibition (\%)} = \frac{\text{Control ODs} - \text{Test ODs}}{\text{Control ODs}} \times 100$$

RESULTS AND DISCUSSION

The synthesis of target hybrids **7a-l** is outlined in **Scheme-I**. Benzimidazole (**1**) was treated with 3-bromopropanenitrile (**2**) in acetonitrile using K_2CO_3 as the base under reflux for 2 h to afford 3-(1*H*-benzo[*d*]imidazol-1-yl)propanenitrile (**3**). The nitrile intermediate **3** was subsequently reacted with thiourea (**4**) and $AlCl_3$ in *n*-butyl acetate, followed by the addition of

molecular iodine, and heated at 70 ºC for 6 h to furnish 3-(2-(1*H*-benzo[*d*]imidazol-1-yl)ethyl)-1,2,4-thiadiazol-5-amine (**5**). The target hybrids **7a-l** were synthesized by coupling amine 5 with the corresponding aromatic carboxylic acids (**6a-l**) in dichloromethane using EDCI and HOBt as coupling agents for 6 h at room temperature, affording the desired products in moderate to good yields.

The structures of the synthesized hybrids were established by ^{1}H NMR, ^{13}C NMR and mass spectrometry. The ^{1}H NMR spectrum of **7a** exhibited a singlet at δ 11.20 ppm and two multiplets at δ 7.89-7.81 and 7.63-7.56 ppm in the aromatic region. The methylene protons appeared as triplets at δ 4.17 and 3.40 ppm. In the ^{13}C NMR spectrum, signals at δ 163.5 and 171.4 ppm were assigned to the carbons of the 1,2,4-thiadiazole ring, while the signal at δ 167.2 ppm corresponded to the amide carbonyl carbon. The mass spectrum displayed a molecular ion peak at *m/z* 350 $[M + H]^+$, consistent with the proposed structure of compound **7a**.

Mechanism: The synthesis proceeds through activation of the nitrile group of N-(2-cyanoethyl)benzimidazole (**1**) by $AlCl_3$, which increases the electrophilicity of the nitrile carbon. Thiosemicarbazide attacks the activated nitrile, followed by proton transfer to afford intermediate **3**. Hydrolysis with H_2O removes aluminium coordination and gives thiosemicarbazide derivative **4**. Treatment with I_2/HI promotes oxidative intramolecular cyclization through the sulfur-containing functionality, forming the five-membered 1,2,4-thiadiazole ring. Dehydrogenation and aromatization furnish intermediate **5**, followed by isolation of amino-substituted benzimidazole–1,2,4-thiadiazole intermediate **6**. Its amino group provides the reactive site for subsequent benzamide formation, affording hybrids **7a-l**. The sequence converts thiosemicarbazide functionality into a rigid heteroaromatic scaffold (**Scheme-II**).

Anti-breast cancer activity: The synthesized compounds were assessed for their anticancer activity against two human breast cancer cell lines MCF-7 and MDA-MB-231 using the MTT assay. The obtained results were compared with standard drug erlotinib. The anticancer results indicate that hybrids **7a-l** displayed moderate to strong cytotoxicity activity with IC_{50} values ranging from 9.10 ± 0.10 μM to 48.23 ± 0.12 μM, while the standard drug has IC_{50} values ranging from 10 ± 0.12 μM to 12.06 ± 0.23 μM. Hybrid **7i** (MCF-7 = 9.30 ± 0.12 and MDA-MB-231 = 9.10 ± 0.10 μM) displayed higher activity as compared to standard drug hybrid and **7j** (MCF-7 = 11.24 ± 0.21 and MDA-MB-231 = 13.08 ± 0.16 μM), hybrid **7k** (MCF-7 = 13.10 ± 0.30 and MDA-MB-231 = 12.10 ± 0.15 μM) and hybrid **7l** (MCF-7 = 14.06 ± 0.12 and MDA-MB-231 = 15.20 ± 0.14 μM) displayed nearer activity as compare to standard erlotinib drug (Table-1).

TABLE-1
ANTI-BREAST ACTIVITY DATA OF SYNTHESIZED HYBRIDS (**7a-l**) WITH IC_{50} IN μM

Hybrids	[b]MCF-7	[c]MDA-MB-231	[d]MCF-10A
7a	45.14 ± 0.04	48.23 ± 0.12	Not tested
7b	42.20 ± 0.10	44.10 ± 0.14	Not tested
7c	40.02 ± 0.06	47.16 ± 0.10	Not tested
7d	38.50 ± 0.10	45.12 ± 0.15	Not tested
7e	32.15 ± 0.07	39.14 ± 0.02	Not tested
7f	34.20 ± 0.17	37.04 ± 0.26	Not tested
7g	29.10 ± 0.08	38.05 ± 0.10	Not tested
7h	18.14 ± 0.13	17.20 ± 0.06	Not tested
7i	9.30 ± 0.12	9.10 ± 0.10	96.20 ± 0.15
7j	11.24 ± 0.21	13.08 ± 0.16	92.10 ± 0.14
7k	13.10 ± 0.30	12.10 ± 0.15	92.20 ± 0.06
7l	14.06 ± 0.12	15.20 ± 0.14	94.02 ± 0.12
Erlotinib	10.00 ± 0.12	12.06 ± 0.23	97.45 ± 0.10

[a]IC_{50} after 26 h of incubation, data are represented as mean ± SD from three different experiments performed in triplicates. [b]MCF-7: human breast cancer cell line. [c]MDA-MB-231: human breast cancer cell line. [c]MCF-10A: Normal breast cancer cell line.

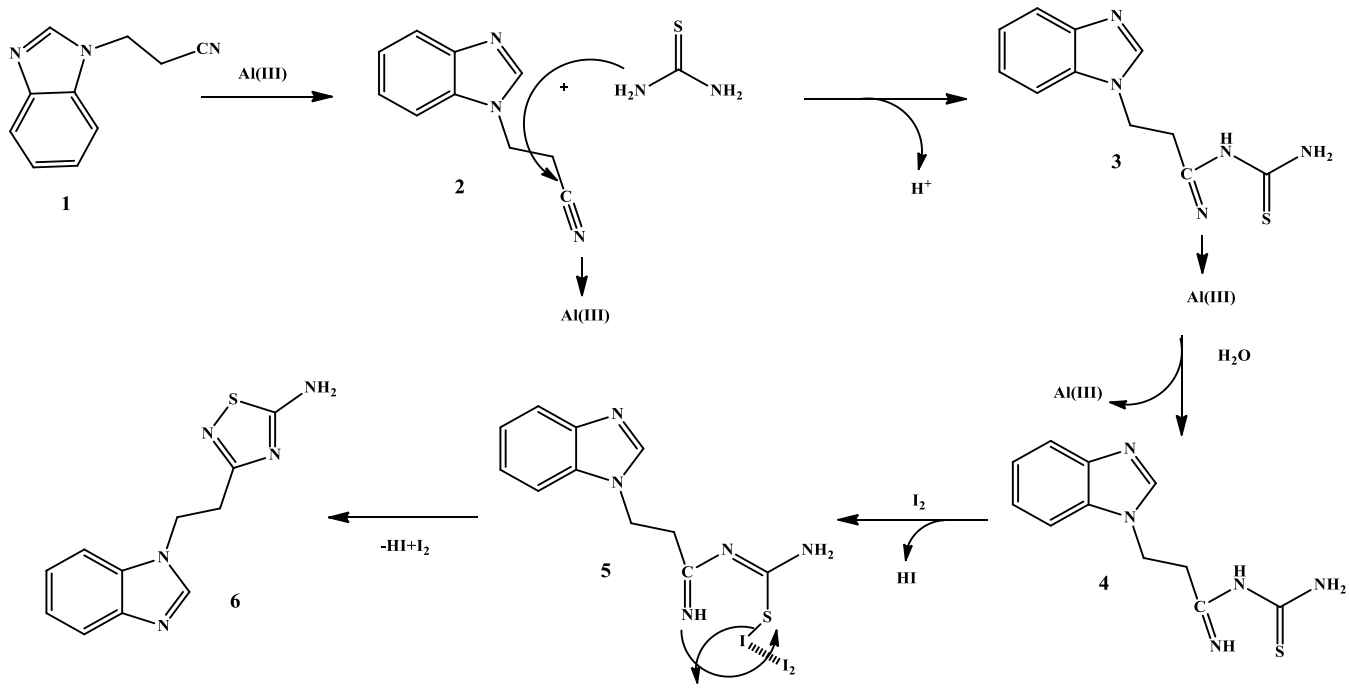

Scheme-II

SAR analysis: The structure–activity relationship (SAR) analysis established a clear influence of the electronic nature and substitution pattern of the phenyl ring on the anticancer activity of hybrids **7a–l**. Among the electron-withdrawing substituents, hybrid **7i**, bearing a strong 4-NO_2 group, exhibited the highest anticancer activity and was more potent than Erlotinib. The 3-NO_2 analogue **7j** showed slightly lower activity than **7i**. Replacement of the nitro group with 4-F in **7k** resulted in a further decrease in activity, while the 4-Cl analogue **7l** displayed lower activity than the other electron-withdrawing derivatives. The 4-CN derivative **7h** retained better activity than the halogen-substituted hybrids. These results indicate that the strong electron-withdrawing nitro group, particularly at the para position, favours anticancer activity within this series.

The electron-donating derivatives exhibited a different activity profile. Hybrid **7f**, bearing methoxy groups at the 3- and 5-positions, showed lower activity than standard erlotinib, while the 4-methoxy analogue **7e** and 3-methoxy analogue **7g** were less active than the nitro-substituted hybrids. The weak electron-donating substituents in **7b-d**, irrespective of their position on the phenyl ring, resulted in markedly reduced activity. Unsubstituted hybrid **7a** displayed the lowest activity among the series. The SAR profile places **7i–l** among the most active derivatives and supports further evaluation of these compounds. Their cytotoxicity toward normal MCF-10A cells was assessed to examine selectivity. Hybrids **7i**, **7j**, **7k** and **7l** exhibited IC_{50} values >97.45 μM, which indicate low cytotoxicity toward the normal cell line.

***in vitro* Tyrosine kinase EGFR inhibitory activity:** The potent hybrids **7i–l** were further evaluated for *in vitro* tyrosine kinase EGFR inhibitory activity, with erlotinib as the reference drug. Hybrids **7i** and **7j** exhibited IC_{50} values of 0.96 ± 0.02 and 0.99 ± 0.02 μM, respectively, compared with 1.26 ± 0.08 μM for erlotinib, establishing their higher EGFR inhibitory potency. Hybrids **7k** and **7l** showed IC_{50} values of 1.56 ± 0.03 and 1.39 ± 0.08 μM, respectively, and were less potent than the reference drug. The stronger EGFR inhibition observed for the nitro-substituted hybrids **7i** and **7j** is consistent with their cellular anticancer activity and supports EGFR inhibition as a plausible contributor to their activity.

Molecular docking studies: Molecular docking studies were performed for hybrids **7i–l** against the EGFR (PDB ID: 1MI7) to rationalize their inhibitory profiles. Hybrid **7l** exhibited the most favourable binding energy (-9.06 kcal/mol) with an inhibition constant of 227.97 nM, forming a hydrogen bond with MET769 at a distance of 1.87 Å. Hybrid **7i** showed a comparable binding energy of -8.96 kcal/mol and an inhibition constant of 272.13 nM. No hydrogen-bond interaction was observed for **7i**, with hydrophobic and van der Waals interactions likely contributing to its favourable binding (Table-2).

Hybrid **7k** exhibited a binding energy of -8.59 kcal/mol and an inhibition constant of 505.18 nM, with a hydrogen bond involving LYS721 at 1.83 Å. Hybrid **7j** showed a weaker binding energy of -7.82 kcal/mol and an inhibition constant of 1.84 μM, forming a hydrogen bond with ASP831 at 1.74 Å. Erlotinib displayed a binding energy of -5.95 kcal/mol and an inhibition constant of 43.64 μM, despite forming three hydrogen bonds with LYS721, MET769 and ARG817. The docking results identify **7l** and **7i** as the strongest predicted EGFR binders, in agreement with their favourable calculated binding energies. When considered with the cellular and EGFR inhibition data, **7i** emerges as the most consistent lead, while **7l** require further investigation based on its highly favourable predicted EGFR binding (Fig. 2).

Conclusion

The benzimidazole-1,2,4-thiadiazole-benzamide hybrids (**7a-l**) were synthesized and evaluated for anticancer activity against MCF-7 and MDA-MB-231 breast cancer cell lines. Hybrid **7i** exhibited the highest anticancer activity in the series and was more potent than the reference drug erlotinib, while compounds **7j**, **7k** and **7l** showed activities close to that of erlotinib. Hybrids **7i** and **7j** displayed stronger EGFR tyrosine kinase inhibition than erlotinib. Molecular docking studies of **7i-l** revealed favourable interactions with EGFR, with **7i** and **7l** exhibiting particularly strong predicted binding affinities. The combined anticancer, EGFR inhibition and docking results identify **7i** as the most promising hybrid of the series and support further investigation of these compounds as potential EGFR-targeted anticancer agents.

ACKNOWLEDGEMENTS

The authors are grateful to the Head, Department of Chemistry, Mahatma Gandhi University, Nalgonda, India for providing laboratory facilities. The authors are also thankful to Director, Indian Institute of Chemical Technology for providing analytical facilities and also thankful to The Head, Department of Biotechnology for biological analysis.

CONFLICT OF INTEREST

The authors declare that there is no conflict of interests regarding the publication of this article.

TABLE-2
MOLECULAR DOCKING INTERACTION PARAMETERS OF COMPOUNDS **7i, 7j, 7k** AND **7l** WITH THE EPIDERMAL GROWTH FACTOR RECEPTOR (PDB ID: 1MI7)

Compound	Binding energy (kcal/mol)	Inhibition constant	Number of hydrogen bonds	Residues involved in hydrogen bonding (bond length in Å)
7i	-8.96	272.13 nM	–	–
7j	-7.82	1.84 μM	1	ASP831 (1.74)
7k	-8.59	505.18 nM	1	LYS721 (1.83)
7l	-9.06	227.97 nM	1	MET769 (1.87)
Erlotinib	-5.95	43.64 μM	3	LYS721 (1.84), MET769 (2.56), ARG817 (2.07)

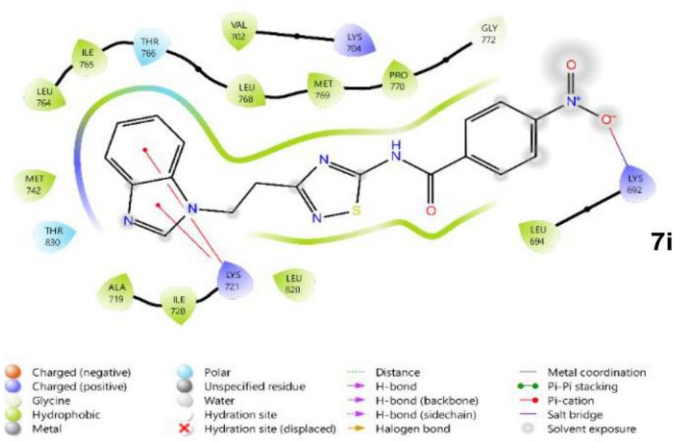
VAL 702
LYS 704
GLY 772
ILE 765
THR 766
LEU 764
LEU 768
MET 769
PRO 770
MET 742
THR 830
LYS 692
LEU 694
ALA 719
ILE 720
LYS 721
LEU 820
7i
Charged (negative)
Charged (positive)
Glycine
Hydrophobic
Metal
Polar
Unspecified residue
Water
Hydration site
Hydration site (displaced)
Distance
H-bond
H-bond (backbone)
H-bond (sidechain)
Halogen bond
Metal coordination
Pi-Pi stacking
Pi-cation
Salt bridge
Solvent exposure

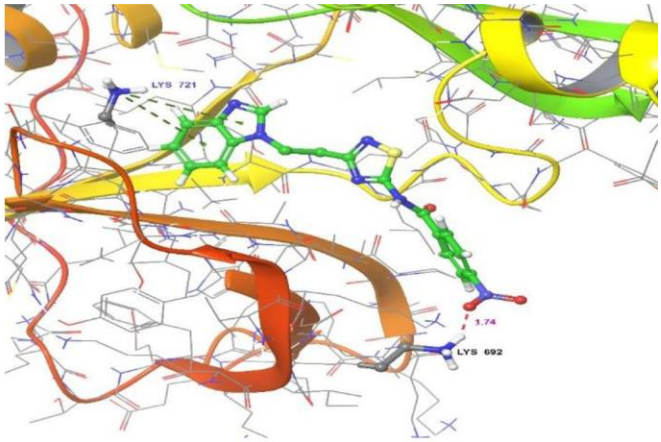
LYS 721
1.74
LYS 692

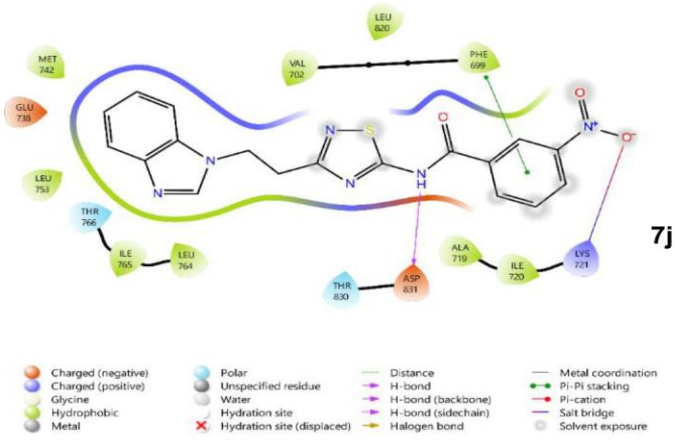
LEU 820
MET 742
VAL 702
PHE 699
GLU 738
LEU 753
THR 766
ILE 765
LEU 764
ALA 719
ILE 720
LYS 721
THR 830
ASP 831
7j
Charged (negative)
Charged (positive)
Glycine
Hydrophobic
Metal
Polar
Unspecified residue
Water
Hydration site
Hydration site (displaced)
Distance
H-bond
H-bond (backbone)
H-bond (sidechain)
Halogen bond
Metal coordination
Pi-Pi stacking
Pi-cation
Salt bridge
Solvent exposure

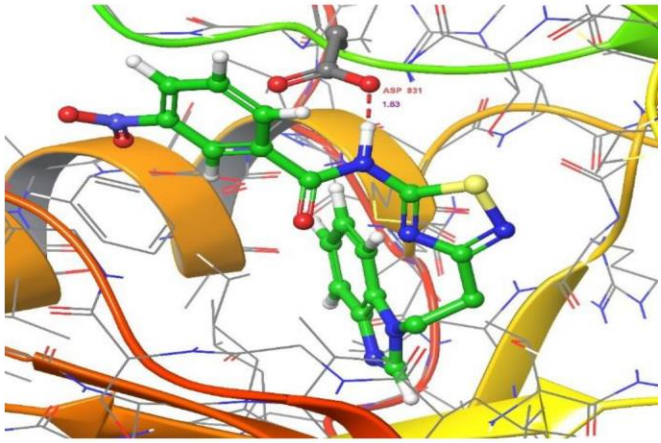
ASP 831
1.83

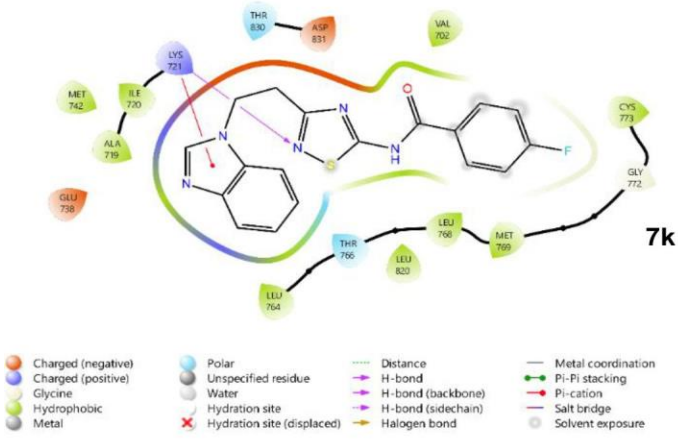
THR 830
ASP 831
VAL 702
LYS 721
MET 742
ILE 720
ALA 719
CYS 773
GLU 738
GLY 772
LEU 768
THR 766
MET 769
LEU 820
LEU 764
7k
Charged (negative)
Charged (positive)
Glycine
Hydrophobic
Metal
Polar
Unspecified residue
Water
Hydration site
Hydration site (displaced)
Distance
H-bond
H-bond (backbone)
H-bond (sidechain)
Halogen bond
Metal coordination
Pi-Pi stacking
Pi-cation
Salt bridge
Solvent exposure

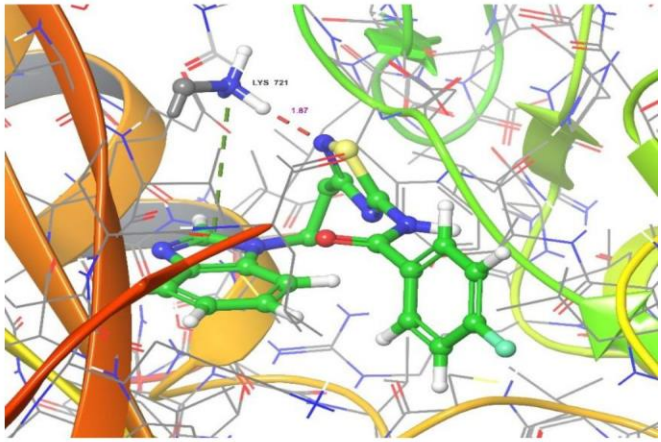
LYS 721
1.87

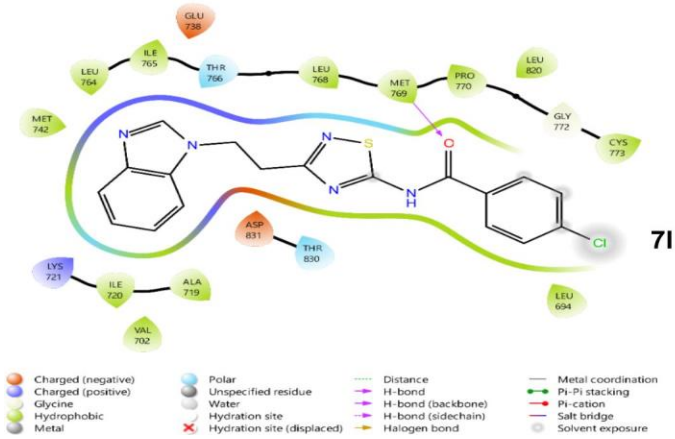
GLU 738
LEU 764
ILE 765
THR 766
LEU 768
MET 769
PRO 770
LEU 820
MET 742
GLY 772
CYS 773
ASP 831
THR 830
LYS 721
ILE 720
ALA 719
LEU 694
VAL 702
7l
Charged (negative)
Charged (positive)
Glycine
Hydrophobic
Metal
Polar
Unspecified residue
Water
Hydration site
Hydration site (displaced)
Distance
H-bond
H-bond (backbone)
H-bond (sidechain)
Halogen bond
Metal coordination
Pi-Pi stacking
Pi-cation
Salt bridge
Solvent exposure

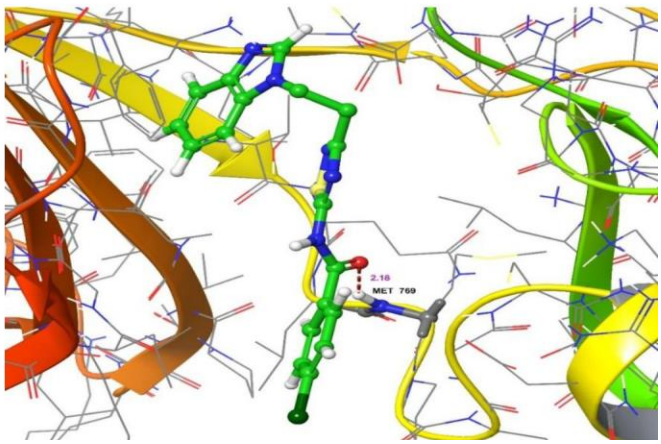
2.18
MET 769

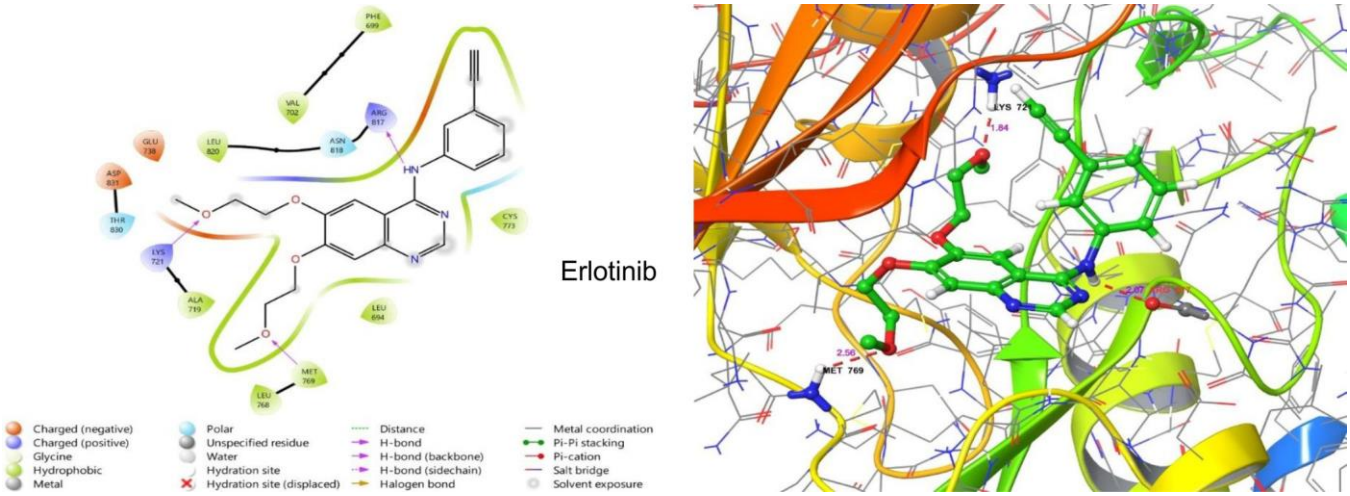

Fig. 1. 2D and 3D poses of hybrids **7i**, **7j**, **7k**, **7l** and erlotinib with EGFR (PDB ID: 1MI7)

DECLARATION OF AI-ASSISTED TECHNOLOGIES

During the preparation of this manuscript, the authors used an AI-assisted tool(s) to improve the language and no data, results or scientific conclusions were generated by AI. All analyses, interpretations and conclusions are the authors' own. The authors reviewed and edited the content and take full responsibility for the published work.

REFERENCES

1. A.J. Robles, S. Mc Cowen, S. Cai, M. Glassman, R.H. Cichewicz, F. Ruiz II, S.F. McHardy and S.L. Mooberry, *J. Med. Chem.*, **60**, 9275 (2017); https://doi.org/10.1021/acs.jmedchem.7b01228
2. N. Shrivastava, M.J. Naim, M.J. Alam, F. Nawaz, S. Ahmed and O. Alam, *Arch. Pharm*, **350**, 201700040 (2017); https://doi.org/10.1002/ardp.201700040
3. V.N. Madia, A. Messore, L. Pescatori, F. Saccoliti, V. Tudino, A. De Leo, M. Bortolami, L. Scipione, R. Costi, S. Rivara, L. Scalvini, M. Mor, F.F. Ferrara, E. Pavoni, G. Roscilli, G. Cassinelli, F.M. Milazzo, G. Battistuzzi, R. Di Santo and G. Giannini, *J. Med. Chem.*, **61**, 6918 (2018); https://doi.org/10.1021/acs.jmedchem.8b00908
4. A. Messore, V.N. Madia, L. Pescatori, F. Saccoliti, V. Tudino, A. De Leo, M. Bortolami, D. De Vita, L. Scipione, F. Pepi, R. Costi, S. Rivara, L. Scalvini, M. Mor, F.F. Ferrara, E. Pavoni, G. Roscilli, G. Cassinelli, F.M. Milazzo, G. Battistuzzi, R. Di Santo and G. Giannini, *J. Med. Chem.*, **61**, 10834 (2018); https://doi.org/10.1021/acs.jmedchem.8b01497
5. R. Reddyrajula, P.V. Kathirvel and N. Shankaraiah, *Bioorg. Med. Chem. Lett.*, **122**, 130167 (2025); https://doi.org/10.1016/j.bmcl.2025.130167
6. P. Suresh, N. Srinivas, V. Ravinder, A. Kamal and K. Shravan Kumar, *Bioorg. Med. Chem. Lett.*, **29**, 2153 (2019); https://doi.org/10.1016/j.bmcl.2019.06.060
7. T.R. Deshmukh, A.P. Sarkate, D.K. Lokwani, S.V. Tiwari, R. Azad and B.B. Shingate, *Bioorg. Med. Chem. Lett.*, **29**, 126618 (2019); https://doi.org/10.1016/j.bmcl.2019.08.022
8. X.-H. Yang, L. Xiang, X. Li, T.-T. Zhao, H. Zhang, W.-P. Zhou, X.-M. Wang, H.-B. Gong and H.-L. Zhu, *Bioorg. Med. Chem.*, **20**, 2789 (2012); https://doi.org/10.1016/j.bmc.2012.03.040
9. C.A.G.N. Montalbetti and V. Falque, *Tetrahedron*, **61**, 10827 (2005); https://doi.org/10.1016/j.tet.2005.08.031
10. J.W. Bode, *Curr. Opin. Drug Discov. Dev.*, **9**, 765 (2006).
11. T. Cupido, J. Tulla-Puche, J. Spengler and F. Albericio, *Curr. Opin. Drug Discov. Dev.*, **10**, 768 (2007).
12. A.K. Ghose, V.N. Viswanadhan and J.J. Wendoloski, *J. Comb. Chem.*, **1**, 55 (1999); https://doi.org/10.1021/cc9800071
13. R.M. Kassab, S.M. Gomha, S.A. Al-Hussain, A.S. Abo Dena, M.M. Abdel-Aziz, M.E.A. Zaki and Z.A. Muhammad, *Arab. J. Chem.*, **14**, 103396 (2021); https://doi.org/10.1016/j.arabjc.2021.103396
14. B.S. Chhikara, N. St. Jean, D. Mandal, A. Kumar and K. Parang, *Eur. J. Med. Chem.*, **46**, 2037 (2011); https://doi.org/10.1016/j.ejmech.2011.02.056
15. A. Ali, D. Bansal, N.K. Kaushik, N. Kaushik, E. Choi and R. Gupta, *J. Chem. Sci.*, **126**, 1091 (2014); https://doi.org/10.1007/s12039-014-0671-3
16. A. Huczyński, G. Klejborowska, M. Antoszczak, E. Maj and J. Wietrzyk, *Bioorg. Med. Chem. Lett.*, **25**, 4539 (2015); https://doi.org/10.1016/j.bmcl.2015.08.067
17. Y. Li, J. Geng, Y. Liu, S. Yu and G. Zhao, *ChemMedChem*, **8**, 27 (2013); https://doi.org/10.1002/cmdc.201200355
18. Z. Wu, F. Xia and R. Lin, *J. Hematol. Oncol.*, **17**, 119 (2024); https://doi.org/10.1186/s 13045-024-01640-8
19. H. Sung, J. Ferlay, R.L. Siegel, M. Laversanne, I. Soerjomataram, A. Jemal and F. Bray, *CA Cancer J. Clin.*, **71**, 209 (2021); https://doi.org/10.3322/caac.21660
20. A. Saini, M. Kuma, S. Bhatt, V. Saini and A. Malik, *Int. J. Pharm. Sci. Res.*, **7**, 3121 (2020); https://doi.org/10.13040/IJPSR.0975-8232.11(7).3109-22
21. S. Morgan, P. Grootendorst, J. Lexchin, C. Cunningham and D. Greyson, *Health Policy*, **100**, 4 (2011); https://doi.org/10.1016/j.healthpol.2010.12.002
22. L. Rong, N. Li and Z. Zhang, *J. Exp. Clin. Cancer Res.*, **41**, 142 (2022); https://doi.org/10.1186/s13046-022-02349-7
23. M.F. Zayed and M.H. Hassan, *Saudi Pharm. J.*, **22**, 157 (2014); https://doi.org/10.1016/j.jsps.2013.03.004
24. D. Zhang, G. Luo, X. Ding and C. Lu, *Acta Pharm. Sin. B*, **2**, 549 (2012); https://doi.org/10.1016/j.apsb.2012.10.004